

For the free diffusion model the explicit expressions for $\lambda_{a,b,\dots}$ and $C_{a,b,\dots}$ used in $J'(\omega)$, eq 3, are for the i th carbon ($i = \beta, \gamma, \delta, \epsilon$).

$$\lambda_{b_1 b_2 \dots b_i} = b_1^2 D_\beta + b_2^2 D_\gamma + \dots + b_i^2 D_i \quad (\text{A1a})$$

$$C_{b_1 b_2 \dots b_i} = (d_{b_1 b_2}^{(2)}(\beta_{12}))^2 (d_{b_2 b_3}^{(2)}(\beta_{23}))^2 \dots (d_{b_{i-1} b_i}^{(2)}(\beta_{i-1 i}))^2 \quad (\text{A1b})$$

The functions $d_{ab}^{(2)}(\beta)$ are elements of the reduced Wigner rotation matrices, b_i are summation indexes taking on values from -2 to $+2$, β_{i-1} are the angles between successive internal rotation axes, all 70.5° , and β_{iF} is the angle between the i th rotation axis and the C^i -H bond, also 70.5° .

The corresponding expressions for the restricted diffusion model are somewhat more complicated and thus each is given separately. For C^β

$$\lambda_{n_1} = n_1^2 \pi^2 D_\beta / 4 \gamma_\beta^2 \quad (\text{A2a})$$

$$C_{b_1 n_1} = \bar{\Gamma}_{b_1 b_1 n_1}(\gamma_\beta) (d_{b_1 0}^{(2)}(\beta_{1F}))^2 \quad (\text{A2b})$$

For C^γ

$$\lambda_{n_1 n_2} = \lambda_{n_1} + n_2^2 \pi^2 D_\gamma / 4 \gamma_\gamma^2 \quad (\text{A3a})$$

$$C_{b_1 b_2 b_2' n_1 n_2} = \bar{\Gamma}_{b_1 b_1 n_1}(\gamma_\beta) d_{b_1 b_2}^{(2)}(\beta_{12}) d_{b_1 b_2'}^{(2)}(\beta_{12}) \bar{\Gamma}_{b_2 b_2' n_2}(\gamma_\gamma) \times \cos [(b_2 - b_2') \alpha_{23}] d_{b_2 0}^{(2)}(\beta_{2F}) d_{b_2' 0}^{(2)}(\beta_{2F}) \quad (\text{A3b})$$

For C^δ

$$\lambda_{n_1 n_2 n_3} = \lambda_{n_1 n_2} + n_3^2 \pi^2 D_\delta / 4 \gamma_\delta^2 \quad (\text{A4a})$$

$$C_{b_1 b_2 b_2' b_3 n_1 n_2 n_3} = \bar{\Gamma}_{b_1 b_1 n_1}(\gamma_\beta) d_{b_1 b_2}^{(2)}(\beta_{12}) d_{b_1 b_2'}^{(2)}(\beta_{12}) \bar{\Gamma}_{b_2 b_2' n_2}(\gamma_\gamma) \times \cos [(b_2 - b_2') \alpha_{23}] d_{b_2 b_3}^{(2)}(\beta_{23}) d_{b_2 b_3'}^{(2)}(\beta_{23}) \bar{\Gamma}_{b_3 b_3 n_3}(\gamma_\delta) (d_{b_3 0}^{(2)}(\beta_{3F}))^2 \quad (\text{A4b})$$

For C^ϵ

$$\lambda_{n_1 n_2 n_3 b_4} = \lambda_{n_1 n_2 n_3} + b_4^2 D_\epsilon \quad (\text{A5a})$$

$$C_{b_1 b_2 b_2' b_3 b_4 n_1 n_2 n_3} = \bar{\Gamma}_{b_1 b_1 n_1}(\gamma_\beta) d_{b_1 b_2}^{(2)}(\beta_{12}) d_{b_1 b_2'}^{(2)}(\beta_{12}) \bar{\Gamma}_{b_2 b_2' n_2}(\gamma_\gamma) \times \cos [(b_2 - b_2') \alpha_{23}] \times d_{b_2 b_3}^{(2)}(\beta_{23}) d_{b_2 b_3'}^{(2)}(\beta_{23}) \bar{\Gamma}_{b_3 b_3 n_3}(\gamma_\delta) (d_{b_3 b_4}^{(2)}(\beta_{34}))^2 (d_{b_3 0}^{(2)}(\beta_{4F}))^2 \quad (\text{A5b})$$

The β angles and b_i summation indexes are as in the free diffusion model, eq A1a and A1b. The functions $\bar{\Gamma}_{bb'n}(\gamma)$ are given in ref 1, eq 3.12b and 3.12c, and the summation indexes used in this study, n_i , can be accurately truncated at $0 \leq n_i \leq 5$ for the amplitudes, γ , used in this study. The angles α_{2F} and α_{23} specify the torsional angles between the C^α - C^β bond and the C^γ -H or C^γ - C^δ bonds, respectively, when viewed along the C^β - C^γ bond with $\gamma_\gamma = 0$. For fluctuations about a trans C^α - C^δ - C^γ - C^δ configuration, $\alpha_{2F} = \pm 120^\circ$ and $\alpha_{23} = 180^\circ$. As one proceeds away from the "stationary" C^α end of the side chain, the torsional angle becomes meaningless if the internal rotations are assumed to be independent. Consequently the torsional angles specifying the angle between the C^δ - C^γ and C^δ -H or C^δ - C^ϵ bonds, α_{3F} and α_{34} , are averaged and do not appear. The angles α_{12} and α_{4F} rigorously do not appear since the motion of C^α is isotropic and that of C^ϵ is unrestricted.

An Electrode Modified with Polymer-Bound Dopamine Which Catalyzes NADH Oxidation

Chantal Degrand*^{1a} and Larry L. Miller*^{1b}

Contribution from the Laboratoire de Polarographie associe au CNRS, Faculte des Sciences Gabriel, 21000 Dijon, France, and the Department of Chemistry, University of Minnesota, Minneapolis, Minnesota 55455. Received March 28, 1980

Abstract: Dopamine was reacted with poly(methacryloyl chloride) producing a modified polymer with hydroquinone functionalities. The loading was 41%. This polymer was dip coated onto a vitreous carbon electrode from pyridine solution. Cyclic voltammetry was performed by using this electrode in buffered 0.1 M aqueous sodium chloride. The hydroquinone moieties could be oxidized to bound quinones in a chemically reversible process. Electrodes with varying amounts of polymer were prepared by varying the concentration of the solution from which the electrode was coated. The current integral indicated that these electrodes held from 0.05 to 0.75 nmol cm^{-2} of electroactive quinone functions. The pH dependence was studied and it was indicated that the hydroquinone moieties had a first $\text{pK}_a \approx 6$. The charging rate was shown to be relatively independent of pH, but dependent on the amount of polymer adsorbed. This modified electrode was used to catalyze the oxidation of NADH. The catalytic efficiency was measured and was shown to conform to stoichiometric expectations. It was demonstrated that the catalytic efficiency increased as the amount of electroactive polymer was increased from 0.05 to 0.2 nmol cm^{-2} but decreased for electrodes holding more polymer.

There is currently great interest in chemically modified electrodes. Of particular importance in the present context are experiments in which electroactive, molecular species, bound to the surface of conductors, are charged and in turn perform redox reactions on solution species.²⁻⁷ This unusual form of electro-

catalysis would seem to have applicability in several fields and the phenomenon raises a number of new, fundamental questions which have not been answered.

In the present work we hoped to provide answers to some of these questions. Particular attention was given to electrodes whose surfaces were coated with polymers^{2b,4-6,8-16} and to pH-dependent

(1) (a) Laboratoire de Polarographie associe au CNRS. (b) University of Minnesota.

(2) (a) Evans, J. F.; Kuwana, T.; Henne, M. T.; Royer, G. P. *J. Electroanal. Chem.* **1977**, *80*, 409. (b) Van De Mark, M. R.; Miller, L. L. *J. Am. Chem. Soc.* **1978**, *100*, 3223.

(3) Tse, D. C. S.; Kuwana, T. *Anal. Chem.* **1978**, *50*, 1315.

(4) Kerr, J. B.; Miller, L. L. *J. Electroanal. Chem.* **1979**, *101*, 263.

(5) For photoinduced examples see: Bolts, J. M.; Wrighton, M. S. *J. Am. Chem. Soc.* **1979**, *101*, 6179. Bocarsly, A. B.; Walton, E. G.; Bradley, M. G.; Wrighton, M. S. *J. Electroanal. Chem.* **1979**, *100*, 283. Bolts, J. M., et al. *J. Am. Chem. Soc.* **1979**, *101*, 1378.

(6) Evans, J. F.; Dautartas, M. F. *J. Electroanal. Chem.*, in press. Evans, J. F., communication.

(7) Kobayashi, N.; Matsue, T.; Fujihira, M.; Osa, T. *J. Electroanal. Chem.* **1979**, *103*, 427.

(8) Kaufman, F. B.; Schroeder, A. H.; Engler, E. M.; Patel, V. V. *J. Am. Chem. Soc.* **1980**, *102*, 483.

(9) Miller, L. L.; Van De Mark, M. R. *J. Am. Chem. Soc.* **1978**, *100*, 639.

(10) Kaufman, F. B.; Engler, E. M. *J. Am. Chem. Soc.* **1979**, *101*, 547.

(11) Doblhofer, K.; Nolte, D.; Ulstrup, J. *Ber. Bunsenges. Phys. Chem.* **1978**, *82*, 403.

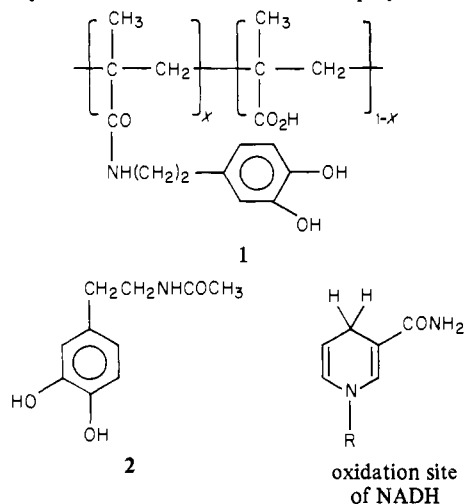
(12) Merz, A.; Bard, A. J. *J. Am. Chem. Soc.* **1978**, *100*, 3222.

redox couples. We chose to study the catalyzed oxidation of the ubiquitous biological reductant dihydronicotinamide adenine dinucleotide (NADH), using an adsorbed, polymer-bound quinone. We anticipated that adsorbed quinoid polymers would give complex electrochemistry which would be difficult to interpret. The polymer layer provides an unusual three-dimensional environment and both proton and electron transfers are required for hydroquinone/quinone interconversion^{17,18} We envisioned, however, some useful applications for such systems which made it worthwhile to accept the complexity.

Direct electrochemical oxidations of NADH have been previously reported.¹⁹ The oxidation has a high activation energy and is complicated by the adsorption of the product, NAD⁺. It is of interest for preparative, mechanistic, and analysis purposes to reduce the activation energy for NADH oxidation and NAD⁺ reduction and for this reason earlier studies have examined oxidations mediated by solution-phase reagents.²⁰ Of special pertinence here, however, is the recent work of Tse and Kuwana³ in which a carbon electrode was modified by covalently binding 3,4-dihydroxybenzylamine to the surface. This electrode was used to catalyze NADH oxidation and, although the electrode was rapidly deactivated, evidence for catalysis was obtained. In light of this work, we chose to prepare a polymer-bound dopamine, adsorb it irreversibly onto a carbon electrode, and investigate the possibility of catalyzing the NADH oxidation. This was successful and, as reported below, the study revealed a number of interesting aspects concerning polymer-modified electrodes and their use as electrocatalysts.

Results and Discussion

The Polymer-Modified Electrode. The polymer **1** was syn-



thesized from dopamine hydrobromide. First, the amine was obtained by treatment with triethylamine in DMF. This DMF solution was reacted with poly(methacryloyl chloride), providing a less soluble polymeric product. The UV and IR spectra of the product were consistent with the proposed structure. Elemental analysis and the UV spectrum showed that the loading was 41%. The first pK_a determined by UV in 40% ethanol/60% water was 8.90.

The polymer **1** was adsorbed onto a vitreous carbon disk (3-mm diameter) by dipping the disk into a dilute (0.002–0.10%) solution

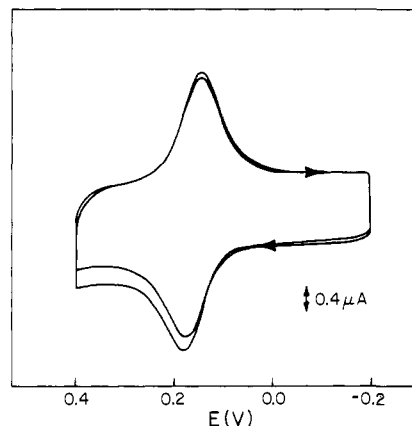


Figure 1. Cyclic voltammogram for El prepared from 0.02% solution of polymer in pyridine. Sweeps 1 and 5 at 46 mV s^{-1} , pH 6.35.

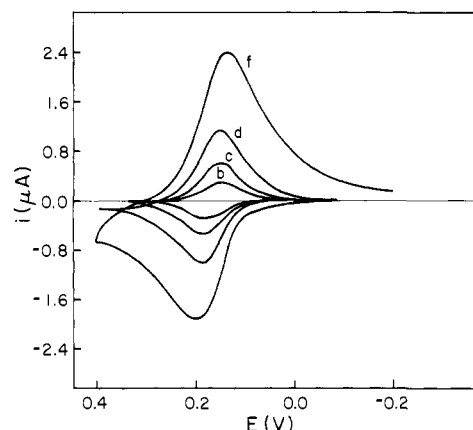


Figure 2. Background subtracted cyclic voltammograms for El with varying Γ (see Table II for Γ values of electrodes b, c, d, and f), 46 mV s^{-1} , pH 6.35.

of **1** in pyridine for 2 min. The electrode was then dried in air. This electrode is designated El. If the carbon surface was properly cleaned, reproducible voltammetric curves could be obtained for an electrode which was repetitively cleaned, dipped, and used. Unless otherwise noted, all the electrochemical experiments used pH 6.35, buffered, aqueous solutions containing 0.1 M NaCl and an SCE reference electrode. An electrode El prepared from a 0.02% solution gave the voltammogram shown in Figure 1 at a sweep rate $\nu = 46 \text{ mV s}^{-1}$. The hydroquinone/quinone couple is evident: $E_p^a = 0.18$, $E_p^c = 0.14$, $\delta_a = \delta_c = 120 \text{ mV}$, where E_p^a is the anodic peak potential, i_p^a is the anodic peak current, and δ_c is the cathodic peak width at half-height. The anodic and cathodic current integrals were nearly equal in every case. This indicated that the quinone form was chemically stable and indicated in this particular case that the 0.02% dip solution gave $0.23 \pm 0.05 \text{ nmol cm}^{-2}$ (assuming $n = 2$) of attached, electroactive quinone functional groups. For comparison a close-packed monolayer of 4-methyl-1,2-dihydroxybenzene "π complexed" on a perfectly flat carbon surface would correspond to 0.6 nmol cm^{-2} .

With continued sweeping of the potential, i_p decayed by about 1%/cycle. The electrode was otherwise stable and could be removed and used in a fresh solution where the first curve was essentially identical with the last made in the previous solution. This stability is in qualitative agreement with the stability of a solution-phase analogue, the amide **2**. Thus, the quinone form of **2** proved to be stable on the 150 mV s^{-1} time scale at pH 7 with $E_p^a = 0.29 \text{ V}$ and $E_p^c = 0.05 \text{ V}$.²¹

Peak shapes for El are more clearly revealed in the background subtracted voltammograms shown in Figure 2. Consider one of these curves. It will be seen that the individual anodic and cathodic

- (13) Itaya, K.; Bard, A. J. *Anal. Chem.* **1978**, *50*, 1487.
 (14) Oyama, N.; Anson, F. C. *J. Am. Chem. Soc.* **1979**, *101*, 739, 2340.
 (15) Nowak, R., et al. *Anal. Chem.* **1980**, *52*, 315.
 (16) Daum, P.; Murray, R. W. *J. Electroanal. Chem.* **1979**, *103*, 289.
 (17) Previous voltammetric studies of adsorbed (monomeric) quinone-hydroquinone couples have appeared. Brown, A. P.; Koval, C.; Anson, F. C. *J. Electroanal. Chem.* **1976**, *72*, 379.
 (18) Takahashi, F.; Aizawa, M.; Kikuchi, R.; Suzuki, S. *Electrochim. Acta* **1977**, *22*, 289, report on a chlorophyll/quinone coated photoelectrode.
 (19) Moiroux, J.; Elving, P. J. *Anal. Chem.* **1979**, *51*, 346. *J. Electroanal. Chem.* **1979**, *102*, 93. Elving, P. J.; Schmamel, C. O.; Santhanam, K. S. V. *Crit. Rev. Anal. Chem.* **1977**, *6*, 1.
 (20) See references cited in Cheng, F. S.; Christian, G. D. *Anal. Chem.* **1977**, *49*, 1785.

- (21) See: Brum, A.; Rosset, R. *J. Electroanal. Chem.* **1974**, *49*, 287, for cyclic voltammetry on dopamine.

Table I. Cyclic Voltammetry Data for EI

Γ , nmol cm ⁻²	pH	ν , mV s ⁻¹	ΔE_p , mV
0.24	6.6	32	35
		46	40
		116	45
		200	50
0.21	9.0	32	20
		46	25
		116	30
		200	40
0.90	6.6	32	70
		46	75
		116	90
		200	120
0.60	9.0	32	40
		46	50
		116	60
		200	85

peaks are not symmetrical about E_p . Each, however, has the same distortion and there is an element of symmetry to the voltammogram. The peak shape is reminiscent of diffusionally controlled cyclic voltammograms. It has recently been reported that a similar voltammogram shape is observed for thick (500–1000 Å) films of "plasma polymerized vinylferrocene" on carbon and the peak shape was attributed to kinetic control by some diffusional phenomenon.¹⁶ In the present case the "film thickness" is unknown, but the total charge indicates very small amounts of polymer.

In Table I are shown $\Delta E_p = E_p^a - E_p^c$, data taken at two different pH values and four sweep rates with electrodes prepared from a 0.02% dip solution. It will be seen that ΔE_p is smaller for slower sweep rates, indicating that the voltammograms are kinetically controlled even at the slow sweep rates. The current returned to zero during the sweep and the surface concentration, Γ , was constant at various sweep rates up to 200 mV s⁻¹. The peak current i_p^a was not, however, linear with ν , because the peaks were broader at high sweep rate.

A quantitative theoretical analysis for voltammetry of polymer-modified electrodes has been put forward.^{22b} This theory differentiates between electron transfer at the polymer-electrode interface and electron transfer through the volume of the adsorbed polymer layer. In qualitative terms it explains that the large ΔE_p and "diffusional tailing" observed for EI can only result if there is slow electron transfer at the interface. If electron transfer at the interface was fast and the rate was only controlled by the reaction rate in the volume of the polymer layer, a small value of ΔE_p was predicted.

It should be further noted that the EI peak shape is quite different from that predicted^{22a} for a situation where the repulsion between adsorbed species determines the shape. This latter situation was encountered in the case of poly-*p*-nitrostyrene on platinum in acetonitrile.²³ In that case and others^{4,11-16} it was observed that at slow sweep rates ΔE_p was independent of ν . Furthermore, the surface charge for these cases was larger. This indicates that the charging rate was faster for poly-*p*-nitrostyrene and the other cases than it is for EI. We suggest that this is due to the slowness of the quinone-hydroquinone chemistry. Indeed, the voltammogram for monomer 2 is also not reversible at $\nu = 50$ mV s⁻¹.

It was of interest, especially in consideration of these slow rates, to investigate the pH dependence of the reactions. It was found that the quinone form of the polymer was not so stable at high pH. This is expected since the quinone is susceptible to nucleophilic attack by hydroxide. This reaction was, however, sufficiently slow that reliable data could be obtained over the pH range 1–10. As shown in Figure 3, ΔE_p is relatively constant at 50–80 mV over the entire pH range when $\nu = 0.1$ V s⁻¹. This suggests that the kinetic slowness is not due to slow proton transfer.

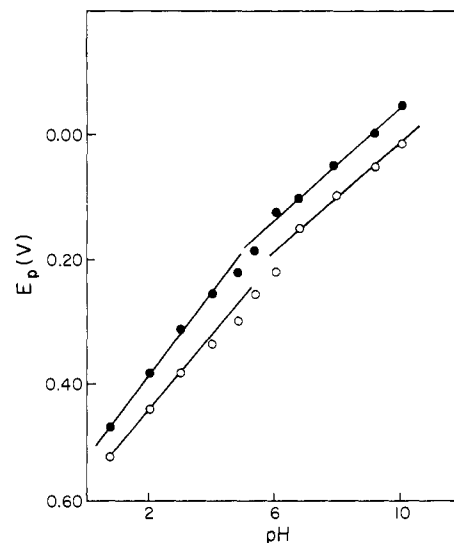
Figure 3. Peak potentials for EI as a function of pH, $\nu = 0.1$ V s⁻¹.

Table II. Electrodes EI

voltammogram ^a	polymer ^b	Γ , nmol cm ⁻² ^c
a	0	0
b	0.002	0.056
c	0.005	0.095
d	0.02	0.23
e	0.05	0.52
f	0.1	0.75

^a See curves in Figures 2 and 5. ^b Weight/volume % of polymer 1 in pyridine solution from which the electrode was prepared.

^c One-half the integrated cyclic voltammetric current for the anodic or cathodic peak corrected for electrode size.

The slope of the E_p vs. pH lines in Figure 3 is 60 mV at low pH. At pH 5 there is a distortion of this linearity and above pH 7 the slope is 40 mV. If one assumes in spite of the irreversibility that the pH dependence follows thermodynamic expectations,^{22,24} it is concluded that $n = 2$ over the entire pH range. Below pH 5 two protons are transferred and above pH 7 one proton is transferred. This indicates that the first hydroquinone $pK_a \approx 6$ for the adsorbed polymer. This value is substantially different from the pK_a for dopamine or the polymer 1 in solution. The difference might be rationalized by consideration of the unusual environment on the surface. Note in particular that the number of electroactive groups is sufficiently small that most or all of them may be in contact with the carbon surface and the pK of these quinones may be quite different from those in solution. We have given this problem further attention in a study of anthraquinone polymers.

Although the electrochemical charging rate as judged by ΔE_p does not appear to be pH dependent, it is highly dependent on the amount of polymer adsorbed. The apparent surface concentration, Γ , will be a direct measure of the amount of bound polymer only if the composition of the adsorbed material is that of the bulk and if all quinone/hydroquinone moieties are electroactive. In any case Γ , measured from a voltammogram where i returns to background, is only a measure of electroactive polymer. By varying the dip solution concentration of 1 in pyridine it was possible to change the amount of polymer adsorbed. As shown in Table II more concentrated solutions gave adsorbed layers which would accept more charge. Figure 2 shows the background subtracted voltammogram shapes for several of these layers. The larger Γ layers showed broader peaks and larger ΔE_p values indicative of slower charging (Table I). Similar changes, but at much higher Γ values, have been previously measured.^{8,9,16}

(22) (a) Laviron, E. *J. Electroanal. Chem.* **1979**, *100*, 263. (b) Laviron, E.; Roullier, L.; Degrand, C., to be published.

(23) Kerr, J. P.; Van De Mark, M. R.; Miller, L. L. *J. Am. Chem. Soc.* **1978**, *102*, 3383.

(24) Gill, R.; Stonehill, H. I. *J. Chem. Soc.* **1952**, 1845. Heyrovsky, J.; Kuta, J. "Principles of Polarography"; Publishing House of the Czechoslovakian Academy of Sciences: Prague, 1965.

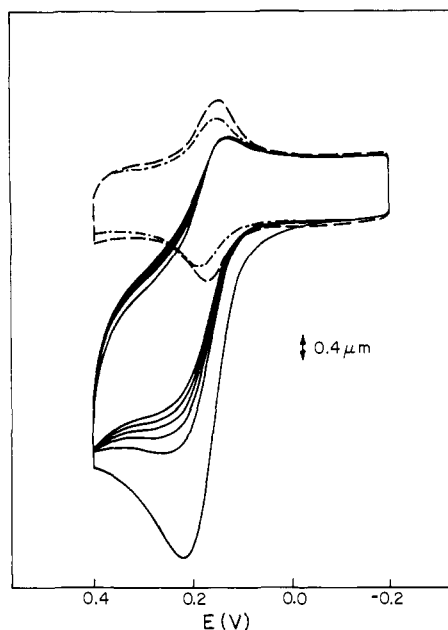


Figure 4. Voltammograms for El, $\Gamma = 0.12 \text{ nmol cm}^{-2}$, $\nu = 46 \text{ mV s}^{-1}$, pH 6.35. El alone, ---; El and 0.5 mM NADH sweeps 1-6, -; El alone after six sweeps with NADH, -.-.

In summary, small Γ layers of hydroquinone polymer 1 can be adsorbed onto carbon and charged with chemical reversibility. The oxidative charging process creates quinone functionalities and the data suggest a first $\text{p}K_a \approx 6$ for the hydroquinone functionalities. The voltammetric responses are kinetically controlled, slow electron transfer at the interface seems important in the charging process, and the rates are noticeably slower for larger Γ layers. Previous studies have not investigated the electrochemistry of adsorbed polymers which require proton as well as electron transfers. The phenomena which have been described here can, however, be largely understood by proposing that classical hydroquinone-quinone electrochemistry is taking place in an unusual environment near the carbon surface.

NADH Oxidations

The oxidation of NADH was performed on clean vitreous carbon and on El. A number of previous studies have described NADH oxidations on carbon electrodes.^{19,25} There are considerable problems with surface deactivation and considerable effort has been expended to develop analytically useful systems. In the present case, reproducible voltammograms for NADH on carbon could only be obtained if the electrode was carefully cleaned and the potential limits were kept constant. These curves were of interest for comparison to the voltammograms for NADH on electrode El. In Figure 4 is shown an example of the substantial catalysis of NADH oxidations achieved by El at pH 6.35 and $\nu = 46 \text{ mV s}^{-1}$. In comparison to the first sweep voltammogram in its absence, 1 mM NADH dramatically enhances the El anodic peak current and depresses the cathodic peak. The second sweep shows smaller currents throughout and by the fifth sweep a steady state is nearly reached. This curve is shown in Figure 4. A background subtracted fifth sweep voltammogram for NADH on clean carbon is shown in Figure 5a. Since NADH on clean carbon gives a very small current at 0.2 V the enhanced anodic current at that potential can be attributed to a catalysis of NADH oxidation by quinone moieties. The most logical general mechanism for this catalysis would utilize the quinone functions as the actual oxidants for incoming NADH molecules. The precise mechanism for *o*-quinone oxidations of NADH is unknown even in homogeneous solution, and will not be speculated upon here.

The quantitative data on such electrocatalytic systems are of considerable interest and in the present case a surprising depen-

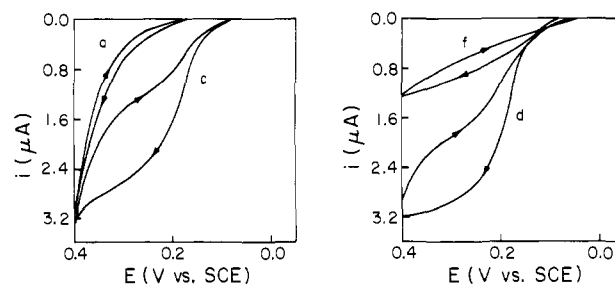


Figure 5. Catalytic currents for 0.5 mM NADH on El with variable Γ , $\Gamma_a = 0.0 \text{ nmol cm}^{-2}$, $\Gamma_c = 0.09 \text{ nmol cm}^{-2}$, $\Gamma_d = 0.23 \text{ nmol cm}^{-2}$, $\Gamma_f = 0.75 \text{ nmol cm}^{-2}$, $\nu = 46 \text{ mV s}^{-1}$, pH 6.35.

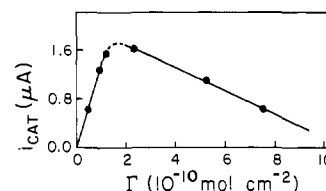


Figure 6. Catalytic efficiencies for El electrodes with varying Γ .

dence of the catalytic efficiency on Γ was discovered. The collection of useful quantitative data required careful control of the experimental variables and restrictive interpretation. It was found, for example, that first sweep currents were dependent on how long the electrode was in the solution. Furthermore, Γ values (as measured by removing the electrodes and putting them into a fresh solution containing no NADH) decayed rapidly with continued sweeping in the presence of NADH ($\sim 25\%$ decrease after five sweeps). It was found that, by keeping the potential limits at -0.2 to 0.4 V and using fifth sweep data, the results could be reproduced. This was convenient because the fifth sweep voltammograms for NADH on clean carbon were also reproducible. The catalytic efficiency was judged by subtracting the voltammogram for El (recorded in a separate solution after the five sweeps with NADH) from that for El plus NADH, giving i_{CAT} vs. E curves. Some of these curves taken at pH 6.35 with 0.5 mM NADH are shown in Figure 5. We define i_{CAT}^p as i_{CAT} measured at the E_p for El alone. Faster sweep rates gave correspondingly smaller i_{CAT}^p . Indeed, for an electrode prepared from 0.02% solution at $\nu > 1 \text{ V s}^{-1}$ and 0.5 mM NADH there is no evidence for catalysis. Over the three-point range 0.25, 0.5, and 1.0 mM, i_{CAT}^p was apparently directly proportional to NADH concentration.

As illustrated in Figure 6 there was a direct proportionality between Γ and i_{CAT}^p over the Γ range $0.05\text{--}0.2 \text{ nmol cm}^{-2}$. Above this Γ value, however, the i_{CAT}^p decreases substantially. This behavior can be rationalized by considering that more sites should enhance the catalytic rate.²⁶ Indeed, the increase in i_{CAT}^p with Γ strongly supports the hypothesis that quinone moieties (or radical precursors to the quinones) are effective mediators for NADH oxidation in a process which has been labeled "EC catalysis". The advantage of more polymer sites must, however, be eventually limited by (1) the rate at which sites can be activated from the underlying carbon surface and (2) the screening of sites near the surface from incoming NADH molecules by polymer lying further away from the underlying surface. We hypothesize that the polymer, especially in the quinone form, is poorly swollen in water and that this limits access of the large NADH to catalytic sites. It is certainly obvious from curve f of Figure 5 that layers with larger Γ also effectively inhibit the "direct" NADH oxidation by limiting access of NADH to the underlying carbon surface sites.²⁷ With small Γ layers it is possible that some NADH is oxidized at the carbon surface and clear evidence for this exists at $E > 0.3 \text{ V}$ on curve c of Figure 5. We note again, however, that E_p for 0.5 mM NADH is about 300 mV anodic of that for El at $\nu = 46 \text{ mV s}^{-1}$. Therefore, it seems unlikely that i_{CAT}^p has much

(26) Andrieux, C. P.; Saveant, J. M. *J. Electroanal. Chem.* **1978**, *93*, 163.

(27) Miller, L. L.; Van De Mark, M. R. *J. Electroanal. Chem.* **1978**, *88*, 437.

contribution from such a process.²⁸

It has been shown²³ in one previous case (nitrostyrene on platinum catalyzing dibromostilbene reduction) that an increase in i_{CAT} occurs as Γ increases, but that this limits at $\Gamma \approx 4 \text{ nmol cm}^{-2}$. The surprising aspect of the present case is that the "limit" where inhibition takes over occurs at such small Γ values. These values correspond to about one close-packed monolayer of monomer. Various explanations for this result can be imagined and some of these will be tested in further studies.

In all the above experiments the first CV sweep was initiated only after the electrode El had been immersed in the buffered NADH solution for several minutes. An intriguing aspect of the kinetics was revealed by an experiment in which the first sweep was initiated as soon as the electrode was immersed. Instead of observing the usual gradual decrease of i_p with successive sweeps, an increase was seen. Thus, background subtracted i_p^a for El in the presence of 1 mM NADH ($\nu = 0.2 \text{ V s}^{-1}$, pH 4.1) was initially 5.8 μA , then 6.6 μA on sweep five and 7.2 μA on sweep ten, and steady state was 7.4 μA . A time-dependent phenomenon of this kind was not observed for El in the absence of NADH. Therefore, we tentatively explain the observation by an initially slow access of NADH to catalyst sites. With time, access to these quinone sites improves and the current increases. We have observed a number of such unexpected time- and/or potential-dependent phenomena with adsorbed polymers and the three-dimensionality of the polymer layers seems responsible.

The success of the NADH catalysis and the unexpected Γ dependence of i_{CAT} make this and related systems of interest for further study. Reports on this work will be forthcoming.

Experimental Section

Cyclic voltammetry was performed by using a PAR Model 173 potentiostat in conjunction with a PAR 175 universal programmer. Voltammograms were recorded on a Varian F-80A x - y recorder. The current integral was measured by the "copy, cut and weigh" method after background subtraction.

(28) Pham, M. C.; Delamar, M.; Lacaze, P. C.; Dubois, J. E. C. *R. Acad. Sci.* 1979, 289, 9, have studied the effect of electroinactive polymer films of the hydroquinone-quinone couple.

NADH was used as received from Sigma Chemical. A fresh solution was prepared for each run and voltammograms were recorded within minutes after the NADH was added. The vitreous carbon was Lorraine V25, 3.0-nm diameter disks sealed to glass. Britton-Robinson buffer solutions were used for pH 2-10. At pH 0.7, 0.2 N H_2SO_4 was used.

The carbon electrodes were cleaned by abrasion with silicon carbide paper (3M brand NH43 600), wiping with a Kimwipe, abrasion with a 0.3- μ alumina on paper disk (ESCIL Type A3), rinsing with water and acetone and air drying, and rinsing with pyridine and air drying. Background CV curves were run, typically from -0.5 to +0.6 V for ten cycles. The electrode was then recleaned by using alumina, water, acetone, air, pyridine, and air and used to record NADH curves or dip coated with polymer. The dip time was generally 2 min in a 0.02% solution (w/v) of 1 in pyridine.

Polymer 1. Dopamine hydrobromide (1.87 g, 8×10^{-3} mol) was dissolved in 2 mL of hot DMF. An equivalent amount of triethylamine was added and the triethylammonium bromide which formed was filtered after addition of 20 mL of acetone. The acetone was evaporated under vacuum and 20 mL of DMF was added. This solution was dried by using alumina, the alumina was filtered off, and the filtrate was added to 209 mg of methacryloyl chloride (Polysciences). After refluxing for 24 h, water was added and a precipitate collected. After careful washing with water 160 mg of beige powder remained. The elemental analysis suggested 41% loading, i.e., $x = 0.41$, $y = 0.59$ in 1, and no chlorine remained in the material. Anal. Calcd: C, 61.4; H, 6.88; N, 4.0. Found: C, 61.52; H, 6.51; N, 4.04. This material is insoluble in acetone and was slightly soluble in pyridine, and shows the expected infrared bands (KBr disk or Nujol mull) from hydroxyl, carboxylic acid, and amide functionalities. In the carbonyl region were bands at 1715 (rel intensity 53), 1660 (65), and 1520 cm^{-1} (49).

The ultraviolet spectrum of the polymer in 40% ethanol/60% water was determined at several pH values. The solution was buffered with 0.1 M Britton-Robinson buffer. In acidic solution the polymer absorbed with λ_{max} 281 nm. Assuming that the loading was 41%, $\log \epsilon$ per hydroquinone unit was 3.54. The monomer dopamine had λ_{max} 280 nm ($\log \epsilon$ 3.45). In basic solution, e.g., pH 10.7, the polymer had λ_{max} 287 nm ($\log \epsilon$ 3.68 per hydroquinone unit). Dopamine at pH 10 had λ_{max} 287 nm ($\log \epsilon$ 3.67). The $\text{p}K_a$ for loss of the first hydroquinone proton from polymer sites was computed from these UV spectra to be 8.90. The dopamine $\text{p}K_a$ was 8.1.

Acknowledgments. This work was supported by the NSF and the CNRS. Travel funds for C.D. were supplied by a NATO fellowship.

Absorption Spectra and Photochemical Rearrangement of Cycloheptatriene Cation to Toluene Cation in Solid Argon

Lester Andrews* and Brian W. Keelan

Contribution from the Chemistry Department, University of Virginia, Charlottesville, Virginia 22901. Received February 4, 1980

Abstract: The toluene and cycloheptatriene cations have been produced and trapped in solid argon by matrix photoionization techniques. Toluene experiments gave a photosensitive 430-nm absorption and weak 480-nm band, the cycloheptatriene studies yielded a broad 480-nm absorption and a weak 430-nm band; these matrix bands are slightly red shifted from the photodissociation spectra (PDS) peaks for the corresponding parent cations. Visible photolysis in cycloheptatriene experiments decreased the 480-nm band and increased the 430-nm absorption, indicating that cycloheptatriene cation can be photochemically rearranged to toluene cation. The toluene cation absorption bandwidth is more than an order of magnitude less in solid argon than in ICR experiments; this may be due to quenching excess vibrational energy in the ground-state ion by the matrix and/or a reduction in the rate of internal conversion from the excited-state ion in the matrix owing to rapid relaxation to lower vibrational levels of the excited state where the density of states for vibronic coupling is less. The reduced photolysis rate of toluene cation in the matrix is consistent with the latter point and an efficient removal of vibrational energy from the vibrationally excited ground-state ion resulting from internal conversion.

Introduction

The toluene radical cation and its dissociation products are among the most widely studied ions in mass and photodissociation spectroscopies. The observation of extensive hydrogen scrambling in mass spectra of isotopically labeled toluenes has prompted

investigation of the possible isomerization of C_7H_8^+ cations produced from toluene and other C_7H_8 compounds. Mass-spectroscopic studies with labeled precursors have been explained by isomerization of the parent cations to a common intermediate for toluene, cycloheptatriene, and norbornadiene.¹⁻⁷ Ion cyclotron